INVESTIGATIONS OF SPACE-CHARGE COMPENSATION IN LOW-ENERGY BEAM TRANSPORT (LEBT) SECTIONS USING A PARTICLE-IN-CELL CODE

D. Noll, M. Droba, O. Meusel, K. Schulte, U. Ratzinger, C. Wiesner,
Institute for Applied Physics, Goethe University, Frankfurt am Main, Germany

Abstract

Among the advantages of magnetostatic LEBT sections in the case of positively charged ion beams is the possibility for compensation of space charge by accumulating electrons. In the past, it has been shown that the distribution of these compensation electrons can lead to unwanted emittance growth [1]. However, the distribution of electrons especially in the presence of the magnetic fields of the focussing lenses is difficult to predict. To improve the understanding of the influence on the beam, models for the relevant processes namely residual gas ionization using realistic cross sections as well as secondary electron production on surfaces have been implemented in a particle-in-cell code. In this contribution, we will present the code used as well as first results for two model systems as an example.

MOTIVATION

Many processes can lead to the appearance of electrons in low-energy ion beams. For low-energy ion beams, the most significant of these are residual gas ionization and secondary particle emission due to beam losses.

A simple estimation of the compensation built-up time by electrons produced via residual gas ionization under the assumption that all electrons can be trapped inside the beam volume leads to

$$t_{\text{compensation}} = \frac{kT}{v_{\text{beam}} p \sigma} = \frac{I}{v_{\text{beam}} e} \nu^{-1} \qquad \nu = \frac{I p \sigma}{e k T}. \quad (1)$$

For a proton beam at 120 keV and a residual gas pressure of $p = 10^{-5}$ mbar N_2 ($\sigma \approx 5\text{Å}^2$) at $T = 300$ K this gives a compensation time of 17 μs. The collision rate is $\nu = 8 \cdot 10^{15}\,\text{s}^{-1}\text{m}^{-1}$.

Secondary electron yields after surface impact for protons at these energies are typically in the order of a few electrons per projectile, strongly depending on surface composition and treatment. For the parameters given above and an electron yield of 2, losses have to be below 0.6% for residual gas ionization to produce more electrons than secondary emission.

For the steady-state however, electrons from residual gas ionization seem to be more relevant since these electrons are born within the beam volume. Furthermore, LEBT sections are typically designed for very low beam loss, even though this might not be the case during the built-up of space charge compensation.

For low-intensity beams, ionization of residual gas by secondary electrons is negligible because the fraction of electrons with energies high enough to lead to ionization is typically small. In the presence of electric fields from a high-intensity particle beam however, electrons can easily gain enough energy for another ionization process to take place. For this reason, the processes $e^- + X \rightarrow X^+ + 2e^-$ should be considered as well.

TEST SYSTEMS

To systematically investigate the built-up of space-charge compensation and the resulting steady-state, a number of test systems were selected.

- A 50 cm drift, 120 keV, 100 mA proton beam with $\epsilon = 100\,\text{mm} \cdot \text{mrad}$. The focussed particle beam was matched using a 2d code so that it enters and leaves the system with the same beam size and maximum divergence angle under full space charge and at 95% global space charge compensation.
- A 80 cm transport section including a solenoid at 378 mT, focussing a divergent proton beam with $\epsilon = 100\,\text{mm} \cdot \text{mrad}$ so that it leaves the system again with same beam size and maximum divergence angle under 95% global compensation.

The systems are fitted with repeller electrodes in the front and the back at negative potential about twice the beam potential in magnitude. Without these, electrons could leave

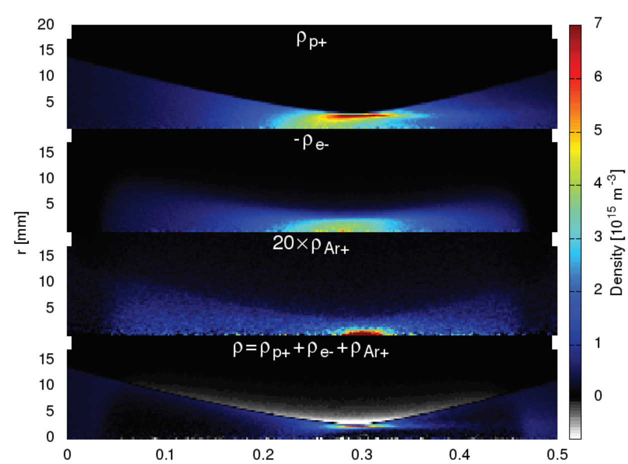

Figure 1: Proton, electron and residual gas ion particle densities in the simulation of the 50cm drift test system. The repeller electrodes at −1.5 kV are visible at the front and the back of the system.

ISBN 978-3-95450-142-7

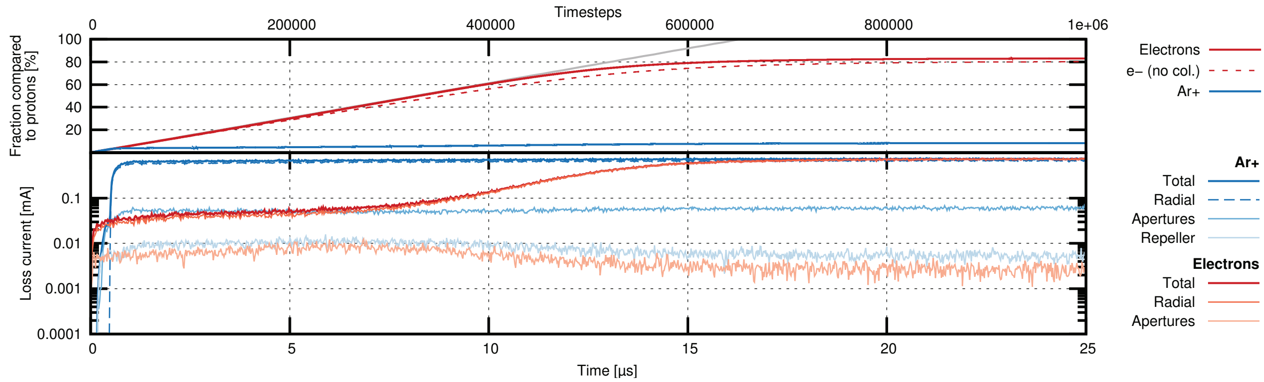

Figure 2: Particle population and losses during the built-up of space-charge compensation for the 50 cm drift system. The compensation degree is plotted for two different simulation runs: with and without electron induced ionization (dashed).

the simulation volume freely. However, this would destroy the controlled environment of the simulation and makes using a fixed beam distribution questionable.

Argon was selected as residual gas as compromise between availability of cross section data, magnitude of cross sections and simplicity of the produced ions. For example, from a review of published data sets, there are more data available for helium and nitrogen. However, the total ionization cross sections for helium are an order of magnitude smaller than for both argon or nitrogen, directly translating in an order of magnitude increased simulation times. Ionization of nitrogen, always present in molecular form, produces either N_2^+ ions or $N + N^+$, which would have to be taken into account.

THE PARTICLE-IN-CELL CODE BENDER

Simulations were done with the 3d particle-in-cell [2] code *bender*. The code provides three solvers for Poisson's equation: a 3d finite-difference Poisson solver which allows handling of boundary conditions on arbitrary geometric objects, an r-z finite-difference solver and a solver using a Fast Fourier Transform. The first solver was used to calculate the electric fields of the repeller electrodes, while the electric self-fields were calculated using either the r-z or the FFT solver.

bender simulates DC beams by inserting slices of beam particles in each timestep, continously building up the beam volume. To exclude switch-on effects resulting from beam particles experiencing the (incomplete) beam potential of the emerging beam, the complete beam was simulated excluding ionization first and then collisions are switched on.

Collisions are handled via the null-collision method [3]. The residual gas is assumed as an ideal gas at constant temperature and pressure.

For proton impact ionization of the residual gas ions, the single differential cross section formula from [4] was used. Single differential cross sections for electron ionization are calculated from the Binary-Encounter-Bethe model [5]. These cross sections provide the distribution of secondary electrons as well as the binding energy of the ionized shell. However, assumptions have to be made for the scattering angle of the projectile particle, the momentum of the remaining ion and the direction of emission of the secondary electron. As a simple model, the secondary electrons were assumed to be isotropically distributed. Furthermore, the remaining ion is assumed to move only in the direction of the incoming projectile. Under these assumptions the remaining quantities can be calculated from energy and momentum conservation.

Both of these assumptions are dubious at best and the results from the model may differ considerably from atomic physics measurements. The model however assures energy and momentum conservation in each simulated collision and reproduces measured electron energy distributions. In the future, more elaborate models including data from double or even triple differential cross sections could be implemented.

RESULTS

Compensation in a Drift Section

Simulations for the drift section were run with 25 ps timesteps using either an r-z mesh with $\Delta r = 0.1$ mm & $\Delta z = 0.2$ mm resolution or a 3d mesh with $\Delta x = \Delta y = 0.4$ mm & $\Delta z = 1.7$ mm.

Figure 2 shows the time development of the global compensation degree and the current of lost particles at the system boundaries. In the first 10 µs the number of electrons increases linearly with the production rate given by (1). Afterwards, the potential of the proton beam is sufficiently reduced and electron losses start to increase until they reach the same level as the losses of residual gas ions. At this point a steady state is reached in which density and velocity distributions remain constant as well. The global degree of space-charge compensation reached is 80.7%, 83.3% if ionizing collisions of electrons are included.

Residual gas ions are accelerated outwards radially by the electric field of the beam and produce a constant current at the beam pipe starting early in the simulation. The energy distribution of these ions could be compared to measurements from residual ion spectrometers. Additionaly, the secondary electron yield of Argon ions in the energy range

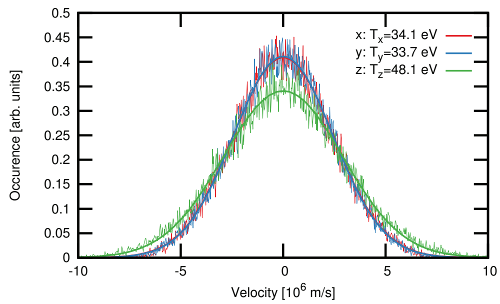

Figure 3: Electron spectrum at the center of the system in the steady-state.

around 100 eV is in the order a few procent [6] for "dirty" surfaces. The influence of the resulting electrons will be investigated in the future.

Figure 3 shows the velocity distribution of a longitudinal slice of trapped electrons at the center of the system. These distributions can be fitted very well with a Gaussian. Generally the temperature in longitudinal direction differs from those in x and y.

The resulting temperatures only show a negligible dependence on simulation parameters like mesh size and total particle count, but differ quantitatively as well as qualitatively in spatial distribution as well as time dependence between the simulations made using the two different Poisson solvers.

Due to their finite temperature the electrons cannot follow the sharp edge of the beam. In Fig. 1, the beam edge can clearly be seen, as well as the halo of electrons outside the beam volume. As a result, in this situation, space charge is not completely compensated locally, even at a high global compensation degree.

The electron column can be considered as a non-neutral plasma confined inside the beam potential. For a slice a the beam focal point, the electron temperature is $T_e = 33.8$ eV, the electron density on axis is $n_{e,max} = 3.9 \cdot 10^{15}$ m^{-3}, the Debye length is $\lambda_d = 0.7$ mm and the plasma frequency is $\omega_p = 3.5$ GHz.

The rms emittance of the beam is increased by about 3 %. The distribution is peaked around the axis – the kurtosis of the distribution increases to 2.25 compared to 2 for the distribution. Also outer particles are focussed a bit less than the beam core.

Compensation in a Single Solenoid

Due to the high magnetic field of the solenoid required to focus the proton beam, the timestep of the simulation had to be decreased to 2 ps. To reduce simulation time, the proton positions are only advanced every 50th, the Argon ions only every 2500th step. Space charge is calculated every 10 steps.

Figure 4 shows particle densities after 35 μs. There is a strong accumulation of electrons on the beam axis and in the solenoid fringe fields. A large fraction of their charge is compensated by residual gas ions which are only slowly accelerated out of the beam volume.

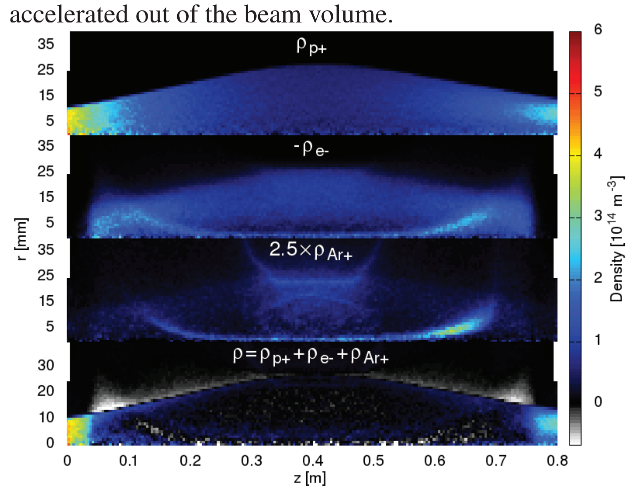

Figure 4: Particle densities for a system containing one solenoid 25 cm long at $B_{max} = 378$ mT.

Inside the solenoid main field, electrons perform cyclotron motion around the magnetic field lines. Thus, even high energy electrons cannot escape the beam volume radially. This leads to improved compensation at the beam edge compared to the situation outside of the solenoid.

OUTLOOK

In future we will include further reactions like secondary electron production on surfaces and atomic excitation and investigate more realistic beam transport sections. Furthermore, when in operation, experiments at the low-energy part of the Frankfurt Neutron Source will allow comparisons between simulation and experiment to be made.

REFERENCES

[1] P. Groß. "Untersuchungen zum Emittanzwachstum intensiver Ionenstrahlen bei teilweise Kompensation der Raumladung." PhD thesis. Goethe Universität Frankfurt am Main, 2000.
[2] R. W. Hockney and J. W. Eastwood. *Computer Simulation Using Particles*. 1981.
[3] V. Vahedi and M. Surendra. "A Monte Carlo collision model for the particle-in-cell method: applications to argon and oxygen discharges." In: *Computer Physics Communications* 87.1–2 (1995), pp. 179–198.
[4] M. E. Rudd et al. "Electron production in proton collisions with atoms and molecules: energy distributions." In: *Reviews of modern physics* 64.2 (1992), p. 441.
[5] Y.-K. Kim and M. E. Rudd. "Binary-encounter-dipole model for electron-impact ionization." In: *Physical Review A* 50.5 (1994), p. 3954.
[6] A. V. Phelps and Z. Lj. Petrovic. "Cold-cathode discharges and breakdown in argon: surface and gas phase production of secondary electrons." In: *Plasma Sources Science and Technology* 8.3 (1999), R21.

ISBN 978-3-95450-142-7